EURODYN 2020
XI International Conference on Structural Dynamics
M. Papadrakakis, M. Fragiadakis, C. Papadimitriou (eds.)
Athens, Greece, 22–24 June 2020

SYSTEM IDENTIFICATION OF HUMAN LEG SPRING STIFFNESS DURING RHYTHMIC JUMPING ON A PERCEPTIBLY MOVING SURFACE

R.E.White[1], N.A.Alexander[2], J.H.G.Macdonald[3]

[1]Department of Civil Engineering, Queen's Building, University of Bristol, UK, BS8 1TR
Rory.White@bristol.ac.uk
[2]Department of Civil Engineering, Queen's Building, University of Bristol, UK, BS8 1TR
Nick.Alexander@bristol.ac.uk
[3]Department of Civil Engineering, Queen's Building, University of Bristol, UK, BS8 1TR
John.Macdonald@bristol.ac.uk

Keywords: pedestrian-loading, biomechanics, non-linear dynamics, human-structure interaction, jumping, experimental system identification

Abstract. In recent years, various man-made structures, such as grandstands and footbridges, have shown significant vibration problems during human jumping causing concern for maintenance and serviceability. To understand the interactions observed between a human and a structure, a 5.5m timber beam was constructed and instrumented. This was designed to simulate a cantilever tier of a grandstand, with similar natural frequency and damping ratio to the full-scale structure and with a similar mass ratio of a single human to the beam as for a crowd to the full-scale structure. Measurements of accelerations and displacements of both the jumper and beam, and of the contact force between them, were acquired. Tests for a range of target jumping frequencies, from below to above the structure's natural frequency, were performed to identify the jumper's dynamics and the induced vibrations of the structure and to observe interactions. System identification techniques were performed to evaluate and model the human leg mechanics of a jumper on a vertically oscillating surface. Force-displacement curves, for both relative (jumper to beam) and absolute displacements, have been obtained. The corresponding leg spring stiffness has been evaluated using a linear fit. Variations in the stiffness for different jumping frequencies is discussed.

1 INTRODUCTION

Previous experimentation into human-structure interaction (HSI) during rhythmic jumping and bobbing on a perceptibly moving surface has shown that periodic jumping close to the natural frequency of the structure was not possible [1,2,3]. A simple reduced-order model [4] was presented to provide an explanation for this problematic jumping. The model assumes an approximate linear spring-mass-damper-actuator system, as an approximation, that is included in IStructE guidelines [4] and other literature [5,6]. Unfortunately, the values of the parameters of the system, are uncertain. Furthermore, a frequency-invariant linear model may not be sufficient. In this paper, force-displacement curves, for absolute and relative displacement, are presented to characterise the leg stiffness from direct measurements of force and displacement. This is performed for low-and high jumping frequencies, above and below a structure's natural frequency. A linear polynomial is applied, using regression analysis, to capture and model the leg stiffness. The evaluated coefficients are observed to be frequency-dependent.

2 EXPERIMENTAL MODELLING

To investigate the interactions of a human jumping rhythmically on a perceptibly moving surface a small beam section was constructed. This was assembled to simulate an oscillating cantilever tier of a grandstand structure due to human jumping loads. These have been known to contain low frequency resonant modes in the region of 1-6Hz with low damping ratios as a result of the long, thin slender structures [7]. This makes them susceptible to significant vertical excitation from humans jumping at various jumping frequencies.

2.1 Beam construction & instrumentation

The beam was designed to be cost effective and simple to construct. The main beam span was constructed from five 150mm x 47mm x 5500mm C24 structural timber beams fixed together side-by-side using thirteen 750mm x 20mm x 100mm plywood slats evenly and symmetrically distributed. This is displayed in Figure 1(a) and 1(b). The beam was clamped at both supports, 75mm from the ends. The clamps were formed from scaffolding pipe tubes, 50mm cross-sectional diameter, cut a length of 900mm. This is shown in Figure 1(c). 10mm holes were drilled into the top and bottom to allow secure fastening of the clamps to the beam using M8 threaded rods. The beam was built into a simple scaffolded system to raise it to provide a clearance of 300mm from the underside of the beam to the finished floor level. This was to ensure that the beam would not make contact with the floor during experimentation. An AMTI OR6-7 force-plate was mounted in the centre of the beam. The total mass of the beam was approximately 170kg. Handrails were constructed for safety of the test subjects. The linear natural frequency and damping ratio of the first bending mode were measured as $f_1=1.89Hz$ and ς_1=0.11%.

Direct measurements of displacement and acceleration of the beam were acquired using two Sétra uniaxial accelerometers and reflective motion capture markers. These were positioned either side of the force plate, across the width of the beam section, at mid-span. The generalised beam dynamics were evaluated by averaging the measurements from each pair of sensors, to evaluate a single measurement for acceleration and displacement respectively.

(a) (b) (c)

Figure 1 Breakdown of constructed bridge (a) Central jumping zone; (b) Length of bridge; (c) Bridge beam end-fixtures

2.2 Procedure and human instrumentation

Biomechanical jumping experiments on the beam were performed for a single male test subject, age 26, mass 74.5kg, height 189cm, leg length 114cm. The test subject's bodyweight corresponded to a human-structure mass ratio of 0.44. Experimental tests were performed above and below the beam's natural frequency. The test subject was given a two-minute rest between each jumping test to ensure that fatigue or physical exhaustion did not occur. Each test were performed over a 50s window with a rhythmic jumping period of 30s. 20s was allowed for the person to step on and off the beam comfortably. Jumping tests were performed at multiple frequencies above and below the beam's natural frequency, (f_1=1.89Hz):1.25Hz, 1.50Hz, 2.70Hz and 3.00Hz.

A 14-marker body system was adopted for the tracking of the human jumping kinematics using Qualisys motion capture software. Markers were fastened using double-sided medical (hypo-allergenic) tape. The test subject wore fitted gym attire to minimise any soft tissue artefacts. From the marker setup, a nine – segment body model was defined following the procedure illustrated by Winter [8] to locate the human body centre of mass (COM) during the tests. This is common practice within the biomechanics research field.

3 DATA PROCESSING

During acquisition of force plate and accelerometer measurements an anti-aliasing low-pass Butterworth filter with a cut-off frequency of 1400Hz was used. The force plate and accelerometer sensor measurements were down-sampled and decimated to the motion capture system's sampling frequency of 100Hz for data processing and analysis. A fourth order low-pass Butterworth filter with a cut-off frequency of 20Hz was applied to all measurements to mitigate any high-frequency noise effects, whilst still capturing higher harmonic responses. Using the 30s jumping record, for each test, a 20s record was extracted for analysis of displacement, acceleration and force data measurements.

The force plate instrumented on the beam measured the loading induced by a human jumper for each target jumping frequency test performed. To quantify the contact force, the inertial force of the force plate itself was first evaluated from a free vibration test. This provided the

'dynamic mass' of the force plate which was found to be 15.3kg. The contact force of the test subject was evaluated as follows:

$$F_{\mathrm{GRF}} = F_{\mathrm{meas}} - m_{fp}\ddot{x}_b \tag{1}$$

where F_{GRF} is the contact force exerted between the test subject and beam, F_{meas} is the directly measured force from the force plate, m_{fp} is the dynamic mass of the force plate, $\ddot{x}_b$ is the measured acceleration at midspan of the beam.

The three-dimensional coordinates of the subject body COM were calculated as follows:

$$\begin{Bmatrix} x_{\mathrm{COM}} \\ y_{\mathrm{COM}} \\ z_{\mathrm{COM}} \end{Bmatrix} = \frac{1}{m_p} \sum_{i=1}^{N_s} m_{\mathrm{seg},i} \begin{Bmatrix} x_{\mathrm{seg},i} \\ y_{\mathrm{seg},i} \\ z_{\mathrm{seg},i} \end{Bmatrix} \tag{2}$$

where x_{COM}, y_{COM}, and z_{COM} are three-dimensional coordinates of the position of the COM of the subject's body, m_p is the subject's total body mass, N_s is the total number of body segments (nine in this case), i is the segment index, $m_{\mathrm{seg},i}$ is the mass of the i-th segment and $x_{\mathrm{seg},i}$, $y_{\mathrm{seg},i}$, and $z_{\mathrm{seg},i}$ are three-dimensional coordinates of the position of the COM of the i-th segment.

Considerable variability in loading/displacement from cycle to cycle was observed in these jumping tests. This is a direct result of the oscillating surface affecting the jumper to be slightly in or out-of-phase with the beam. One consequence was a difficulty in defining, based on period, the flight and contact phases. In order to distinguish the flight and contact phases of the jump cycle, and to allow for noise on the force measurements, the times of take-off and landing were defined as when the contact force equalled 5% of the bodyweight. Smaller values were zeroed as they were assumed to be during the flight phase.

Figure 2 depicts a time-history breakdown for the test subject's dynamics of a test at their preferred jumping frequency. Figure 2(a) indicates the jumper's body segments and centre-of-mass trajectories, as described in Eq.2. This is detailed as grey and black respectively. Figure 2(b) shows the processed contact force to distinguish clear contact and flight phases, normalised to the person's bodyweight. Figure 2(c) displays the beam mid-span displacement. The positive sign convention for the jumper COM and beam displacements are defined as the downward displacement corresponding to a positive contact force indicating compression. The reference (zero) displacement for the jumper is defined as the static COM displacement. These measurements are processed further into overlaid cycle-by-cycle time-histories to signify the jumper's variability performing rhythmic jumping on the oscillating beam, as shown in Figure 3.

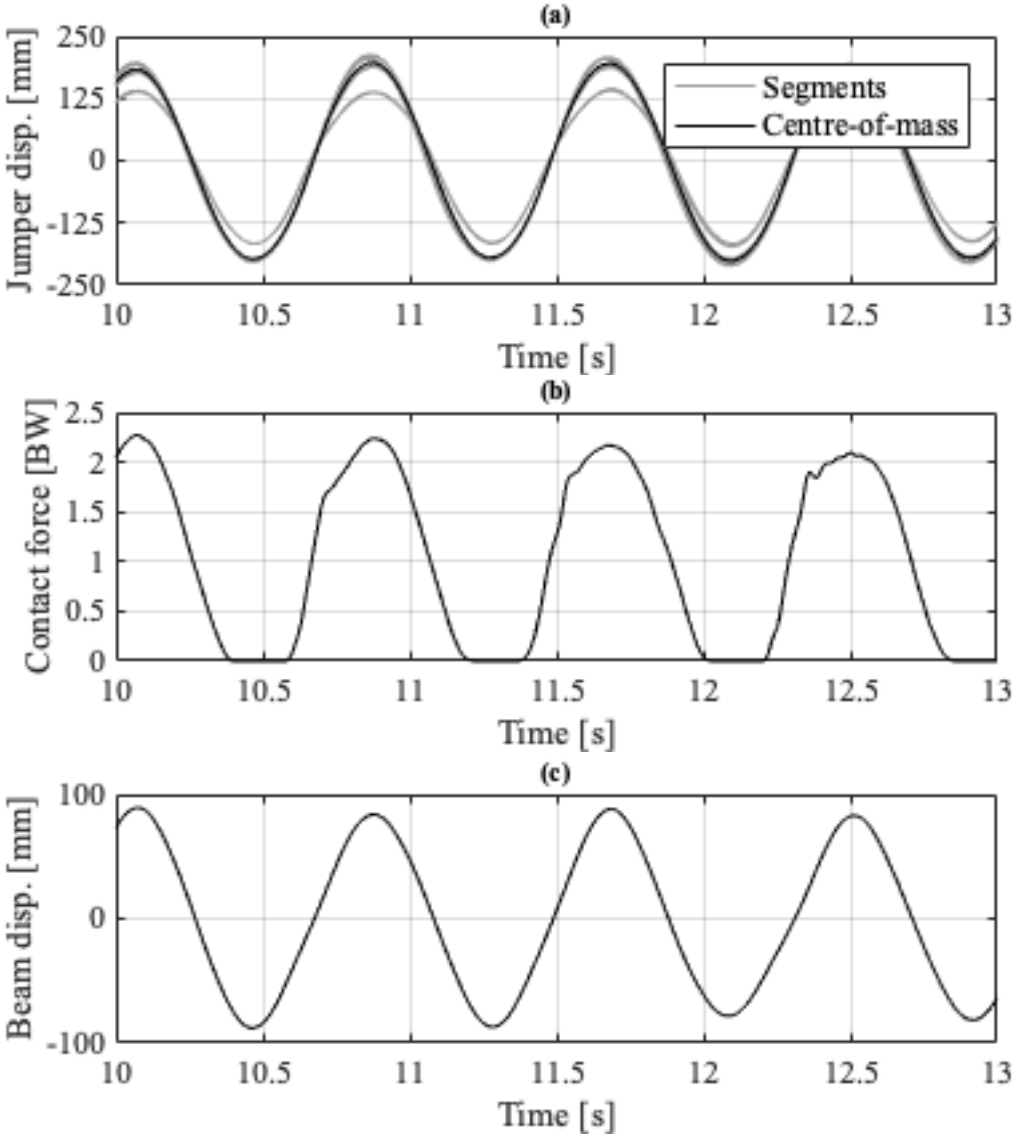

Figure 2 Example time-histories of test subject's dynamics jumping at their preferred frequency (a) jumper COM (grey indicates the defined body segment trajectories and black indicates the evaluated centre-of-mass); (b) Contact force; (c) Beam mid-span displacement

Figure 3 displays the time-histories of the contact force (a), relative displacement (b), jumper to bridge, jumper COM displacement (c) and beam displacement (d) for a test at the test subject's preferred jumping frequency. The relative displacement is defined as the jumper COM to bridge displacement. The mean achieved jumping frequency for this test was found to be 1.26 ± 0.05Hz. A jumping cycle is characterised by the contact and flight phases. These are indicated in Figure 3 as a comparative measure of the time spent and response shape for each phase. The dashed grey lines indicate approximate contact and flight phases. For this specific test, the contact phase is observed to be the majority of the period of oscillation and displays significant deflection of both the jumper and beam resulting in a large relative displacement (leg compression).

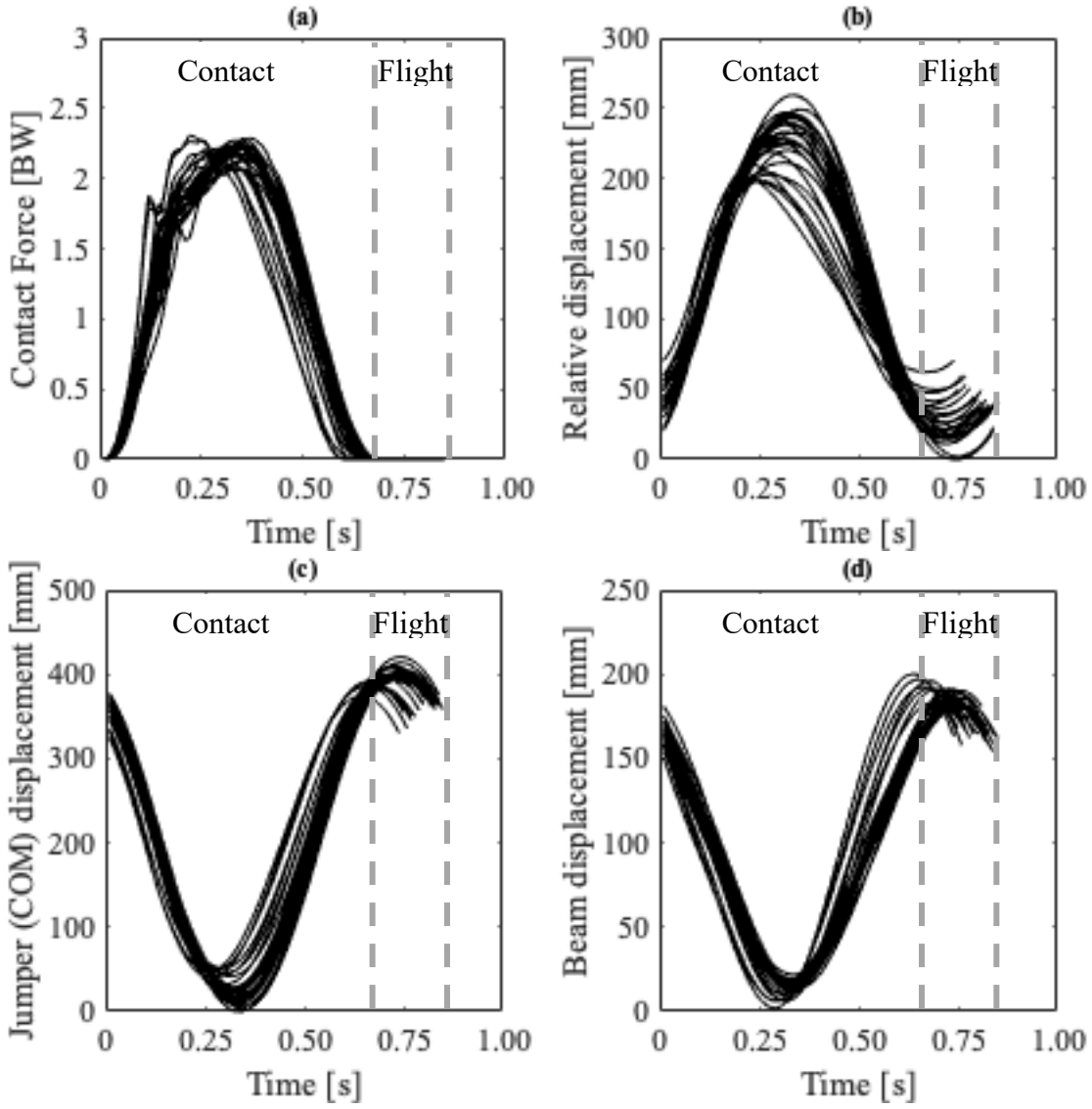

Figure 3 Example time-histories of test subject jumping at their preferred frequency, mean 1.26Hz (a) Contact force; (b) Relative displacement; (c) Jumper centre-of-mass displacement; (d) Beam centre-of-mass displacement

Table 1 summarises the dynamics observed during jumping tests above and below the structure's natural frequency. These are evaluated as the mean peak values observed for each test case. The peak contact force is normalised to the test subject's bodyweight, BW.

Jumping frequency [Hz]	Displacement (mm)			Beam acceleration (m/s^2)	Peak contact force (BW)
	Jumper centre-of-mass	Beam	Relative		
1.26	216	106	125.42	9.56	2.36
1.50	172	151	321.25	14.21	2.91
2.70	105	55.8	137	12.7	3.00
3.00	52.9	37.8	91.9	13.97	3.05

Table 1 Summary of mean peak values of dynamics measured for jumping frequency test cases above and below the structure's natural frequency (f_1=1.89Hz)

4 FORCE-DISPLACEMENT CURVES

Force-displacement curves for the coupled oscillating jumper and beam system have been plotted for the absolute (jumper's COM) and relative displacement (jumper to bridge). This is performed as a comparison to explore the leg stiffness effects for each case to understand the underlying interactions.

The compressing and extending stages of the contact phase were identified for each jumping test case to examine the loading and unloading relationships. These are overlaid in Figures 4 and 5. The red dots denote compressing, whilst blue indicates extending. This was important to understand any subtle changes in the leg stiffness during each stage of the contact phase. In order to distinguish the compressing and extending stages during the contact phase, the velocity was evaluated, for each displacement measurement, to identify the loading conditions. To be consistent with the positive sign convention of downward displacement, corresponding to a positive contact force, compressing was defined as positive velocity, whilst extending was defined as negative velocity.

A simple linear relationship, Eq.(5), was applied to each jumping test case, for both displacements, to characterise the leg stiffness profile during the compression and extension stages of the contact phase.

$$F_{GRF} = kZ \tag{3}$$

Where k is the linear stiffness coefficient of Eq.(5) and Z is the displacement of interest (absolute or relative). These were found using regression analysis.

4.1 Relative displacement

Figure 4 displays the force-displacement curves for jumping at 1.25Hz, 1.50Hz, 2.70Hz and 3.00Hz, using the measured relative displacement. Below the structure's natural frequency (f_1=1.89Hz), the 1.25Hz and 1.50Hz test cases indicate large relative displacements with similar contact forces. The shapes are observed as being approximately linear with the compressing and extending stages following very similar paths indicating similar stiffness. For the 1.50Hz test case, the compressing stage of the cycle is seen to be considerably variable. Table 1 indicates that the beam displacement amplitude is largest at the 1.50Hz which could be due to a jumping frequency near resonance.

Above the structure's natural frequency, the 2.70Hz and 3.00Hz cases indicate less deflection (approximately 200mm max displacement corresponding to 2kN of force, 2.36BW). Interestingly, both curves of these test cases display hysteresis loops indicating that the energy exchanged during the leg compression and extension is significantly different. The stiffness

profiles during each stage of contact are observed to be considerably different suggesting a larger stiffness spring during compression in comparison to extension.

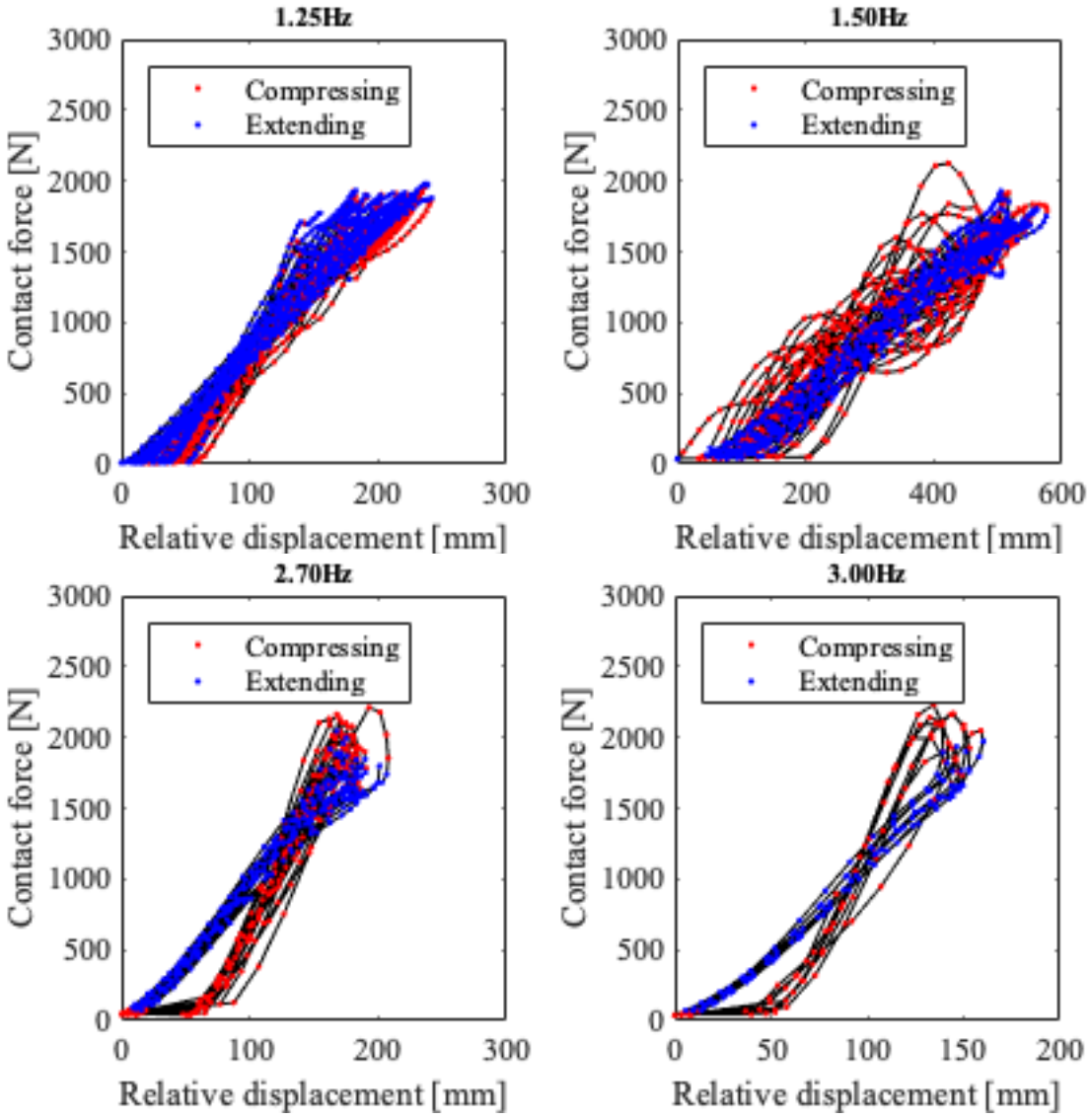

Figure 4 Contact force - relative displacement relationships for jumping frequencies above and below the structure's natural frequency (f_1=1.89Hz). Red dots denote compression, whilst blue indicates extension.

4.2 Absolute displacement

Figure 5 displays the force-displacement curves for jumping at 1.25Hz, 1.50Hz, 2.70Hz and 3.00Hz, using the measured jumper's COM displacement. Below the structure's natural frequency (f_1=1.89Hz), the jumper's COM observes large displacements, approximately 300mm max deflections corresponding to 2kN of force (a bodyweight factor of 2.36). The 1.25Hz test case shows a clear linear trend with the compressing and extending stages following very similar paths. The 1.50Hz jumping is rather variable, particularly during compression, suggesting the test subject found this frequency difficult to periodically jump at. The extension is observed to be clearly linear.

For the 2.70Hz test case, the trend does look linear but, similarly to the relative displacement curve for this test exhibits a hysteresis loop, there is tentative evidence that this may be subtly observed for the absolute displacement. This is suggestive for the compressing and extending stages for this test indicating slightly different leg stiffnesses. At 3.00Hz, the force-displacement curve observes a subtle hysteresis loop, mirroring the effects of the relative displacement case. The compressing and extending stages follow distinctly different paths corresponding to distinctive stiffness profiles. The relationship during extension is observed to be linear in comparison to compression which is clearly complex in nature.

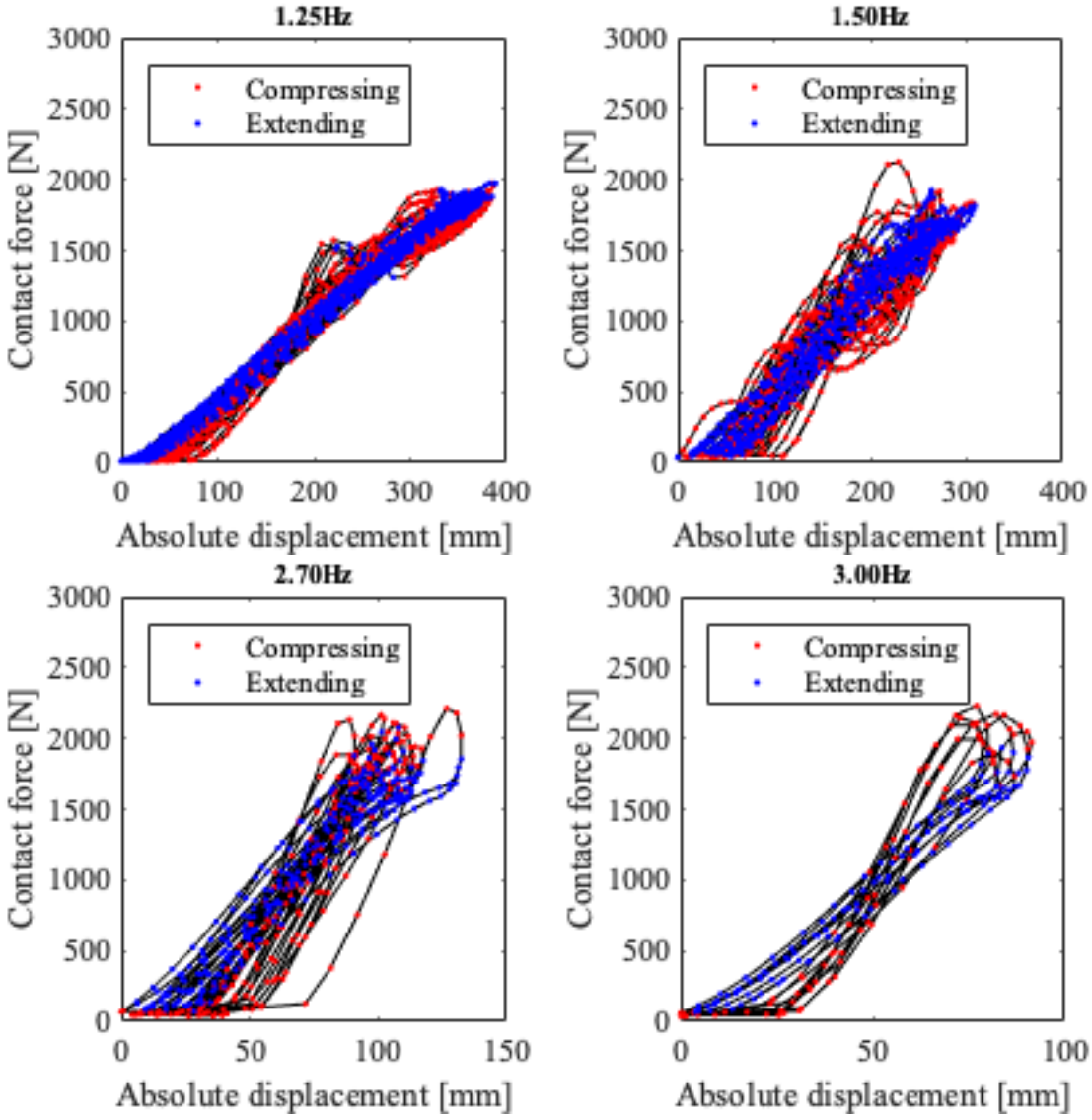

Figure 5 Contact force - absolute displacement relationships for jumping frequencies above and below the structure's natural frequency (f_1=1.89Hz). Red dots denote compression, blue dots indicate extension.

5 LEG STIFFNESS

Figure 6 displays the frequency-dependency of the linear fits. The compression stiffness coefficients are indicated as red crosses whilst the extension stiffness coefficients are presented

as blue circles. The leg stiffness coefficients, displayed in Figure 6, are computed using the calculated stiffness coefficients, in Figures 4 and 5, divided by the test subject's body mass. The stiffness coefficients evaluated from the relative and absolute displacements are represented in Figure 6(a) and 6(b) respectively. In Figure 6(a), the compressing and extending stiffness are seen to increase at high frequency jumping whilst the stiffness indicates a decrease from 1.25Hz to 1.50Hz. The rates of increase for the stiffness coefficients are suggestive of being non-linear. Figure 6(b) displays an increase in stiffness from 1.25Hz to 1.50Hz followed by an increase in 2.70Hz to 3.00Hz. The compressing stiffness at these frequencies increase significantly in comparison to the extending stiffness. At low jumping frequencies, the stiffness coefficients for the two stages, obtained for both absolute and relative displacement, are approximately the same in value. Above the structure's natural frequency (f_1=1.89Hz), the compressing and extending stiffness coefficients are observed to differ considerably indicating a complex stiffness mechanism of the leg. This is more evident in the case of the absolute displacement, Figure 6(b).

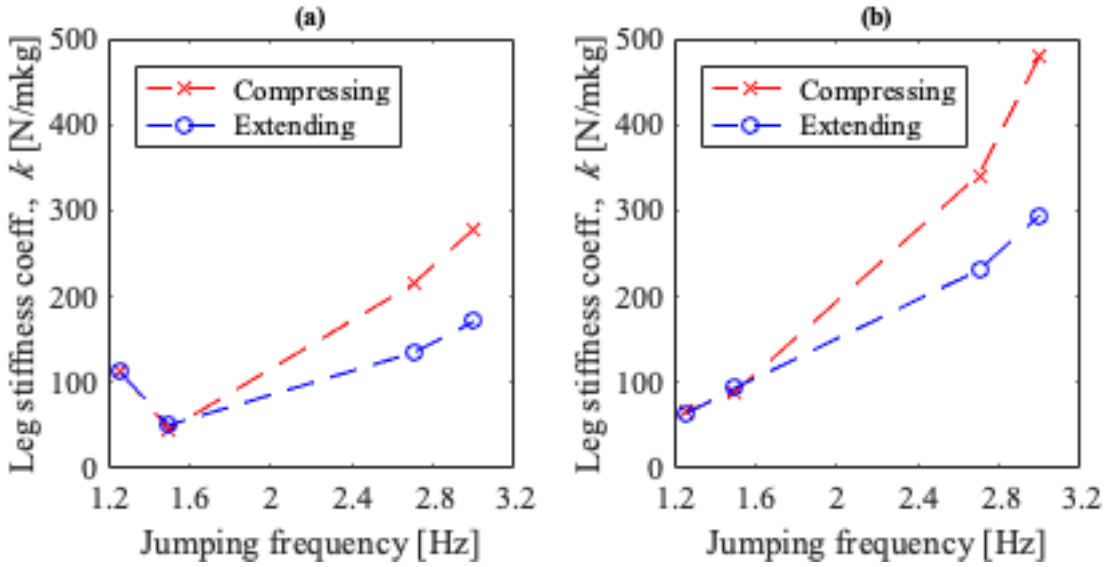

Figure 6 Frequency dependency of linear stiffness coefficients (a) relative displacement; (b) absolute displacement

6 CONCLUSIONS

Force-deflection curves for absolute and relative displacement measurements have been presented with the corresponding stiffness profile being explored. At low jumping frequencies, the force-displacement relationships are observed to be close to pseudo-linear. However, at high jumping frequencies, the relationships are observed to be more complex. The relative displacement exhibits hysteresis loops, indicating a complex energy exchange at high frequency jumping. Hysteresis is subtly mirrored in the absolute displacement case for the 3.00Hz jumping case. The frequency-dependencies of the stiffness coefficients suggest that at low jumping frequencies the stiffness profile during compression and extension are extremely similar. At high jumping frequencies, the stiffness is observed to be larger and complex during compression in comparison to extension. This suggests that the leg stiffness mechanism is considerably more complex at high jumping frequencies.

REFERENCES

[1] Yao S, Wright JR, Pavic A, Reynolds P. Experimental study of human-induced dynamic forces due to jumping on a perceptibly moving structure. Journal of Sound and Vibration. 2006;296(1-2):150-65.

[2] Yao S, Wright JR, Pavic A, Reynolds P. Experimental study of human-induced dynamic forces due to bouncing on a perceptibly moving structure. Canadian Journal of Civil Engineering. 2004;31(6):1109-18.

[3] Harrison RE, Yao S, Wright JR, Pavic A, Reynolds P. Human jumping and bobbing forces on flexible structures: effect of structural properties. Journal of Engineering Mechanics. 2008;134(8):663-75.

[4] IStructE, Dynamic performance requirements for permanent grandstands subject to crowd action, The Institution of Structural Engineers, London, 2008

[5] Alexander NA, Macdonald JHG, Champneys AR. Numerical investigation of a simple model of human jumping on an oscillating structure. Procedia engineering. 2017 ;199:2844-9.

[6] N.A. Alexander, Theoretical treatment of crowd-structure interaction dynamics, Proceedings of the Institution of Civil Engineers - Structures and Buildings, 2006, 159(6), 329-338

[7] J.W. Dougill, J.R. Wright, J.G. Parkhouse and R.E. Harrison, Human structure interaction during rhythmic bobbing, The Structural Engineer, 2006, 84:32-39

[8] Winter DA. Biomechanics and motor control of human movement. John Wiley & Sons; 2009